



Surface-displayed phenolic acid decarboxylase for increased vinylphenolic pyranoanthocyanins in blueberry wine

Huaili Deng^a, Qiuya Gu^a, Xiaobin Yu^{a,**}, Jianli Zhou^{b,***}, Xiaobo Liu^{c,*}

^a Key Laboratory of Carbohydrate Chemistry and Biotechnology, Ministry of Education, Jiangnan University, 1800 Lihu Road, Wuxi, 214122, China

^b Key Laboratory of Plant Resource Conservation and Germplasm Innovation in Mountainous Region (Ministry of Education), School of Liquor and Food Engineering, Guizhou University, Guiyang, 550025, China

^c School of Environmental and Biological Engineering, Nanjing University of Science and Technology, 200 Xiaolingwei Street, Nanjing, 210094, China

ARTICLE INFO

Handling editor: Siyun Wang

Keywords:

Color stability
HPLC/ESI-MS
Fruit wine
4-Vinyl derivatives

ABSTRACT

During the fruit wine production, phenolic acid decarboxylase (PAD) converts free hydroxycinnamic acid into 4-vinyl derivatives that can then react spontaneously with anthocyanins, generating more stable pyranoanthocyanins that are responsible for the color stability of fruit wine. Nevertheless, the low PAD activity in yeast under the winemaking conditions has largely limited the generation of 4-vinyl derivatives. To bridge this gap, we expressed PAD from *Bacillus amyloliquefaciens* in *Pichia pastoris* and surface-displayed it on *Saccharomyces cerevisiae*. As a result, *S. cerevisiae* surface-displayed PAD (SDPAD) exhibited an enhanced thermal stability and tolerance to acidic conditions. Fermentation experiments showed that SDPAD can significantly increase the content of vinylphenolic pyranoanthocyanins and thus maintain the color stability of blueberry wine. Our study demonstrated the feasibility of surface display technology for color stability enhancement during the production of blueberry wine, providing a new and effective solution to increase the content of vinylphenolic pyranoanthocyanins in the fruit-based wines.

1. Introduction

The color of wine, which is fermented using fruits, is one of the most important sensory characteristics perceived by consumers. The abundant anthocyanins in many fruits are the primary contributors to the color of fruit wine products (Gao et al., 2023). However, anthocyanins have limited stability, leading to co-pigmentation, polymerization, degradation, and color change in fruit wine during processing and aging (De Freitas and Mateus, 2011). During the wine-making process of fruit wine, secondary small molecules (pyruvic acid, acetaldehyde, etc.) of carbohydrate metabolisms and hydroxycinnamic acids (p-Coumaric acid, ferulic acid, caffeic acid, etc.) can react with anthocyanins to generate different types of pyranoanthocyanins after decarboxylation reaction (Lu et al., 2000). Pyranoanthocyanins contribute to a stronger color stability, antioxidant properties and acidity stability (Sun et al., 2020). Currently, different types of pyranoanthocyanins, including Vitisins A/B type, Pinotin A/B type, phenolic type, and methyl type have

been identified (Oliveira et al., 2007). Among them, vinylphenolic pyranoanthocyanins are formed from hydroxycinnamic acid after being decarboxylated by phenolic acid decarboxylase (PAD), which can improve the color stability of fruit wine because PAD can effectively promotes the formation of 4-vinyl derivatives (Benito et al., 2011). Thus, PAD plays a crucial role in the formation of vinylphenolic pyranoanthocyanins during the reaction (Morata et al., 2021).

PAD is an enzyme that can break down phenolic acids to produce 4-vinyl derivatives through the non-oxidative decarboxylation reaction (Sheng et al., 2015). In yeast, hydroxycinnamic acid decarboxylase (HCDC) is the enzyme with the same catalytic function as PAD in bacteria. Its substrate is mainly hydroxycinnamic acid with cinnamic acid as the core in phenolic acids and a C₆-C₃ skeleton. Although the two enzymes have similar amino acid sequences, HCDC requires a cofactor flavin mononucleotide (FMN) and has low catalytic activity, while bacterial PAD has high catalytic activity and stability (Jung et al., 2013). Moreover, most of the HCDC directly used in alcoholic beverages usually

* Corresponding author. School of Environmental and Biological Engineering, Nanjing University of Science and Technology, 200 Xiaolingwei Street, Nanjing, Jiangsu, 210094, China.

** Corresponding author. School of Biotechnology, Jiangnan University, 1800 Lihu Road, Wuxi, 214122, China.

*** Corresponding author. School of Liquor and Food Engineering, Guizhou University, Huaxi District, Guiyang, 550025, China.

E-mail addresses: xbyu@jiangnan.edu.cn (X. Yu), zhoujl@gzu.edu.cn (J. Zhou), xbliu@njust.edu.cn (X. Liu).

<https://doi.org/10.1016/j.crfs.2024.100730>

Received 3 December 2023; Received in revised form 25 March 2024; Accepted 2 April 2024

Available online 7 April 2024

2665-9271/© 2024 The Author(s). Published by Elsevier B.V. This is an open access article under the CC BY-NC-ND license (<http://creativecommons.org/licenses/by-nc-nd/4.0/>).

lose the catalytic function due to the impacts of low pH and alcohol during the brewing process (Lentz, 2018). Therefore, developing a yeast with high decarboxylation ability and strong tolerance to the brewing environment of fruit wine becomes a new solution to improve the content of vinylphenolic pyranoanthocyanins in fruit wine and the color stability of fruit wine.

In recent years, display of active enzymes on the cell surface becomes an alternative to classic enzyme immobilization for retention of high catalytic activity. The surface display of enzymes on the yeast surface is a whole-cell catalyst that can self-fix on the surface of microorganisms, thus avoiding laborious purification and immobilization (Kondo and Ueda, 2004). Yeast surface-displayed PAD have attracted great interest because their post-translational modification mechanisms are generally considered safe, compared to prokaryotic expression systems (Çelik and Çalik, 2012). However, *Saccharomyces cerevisiae* surface-displayed PAD as a whole-cell catalyst for conversion of hydroxycinnamic acids has not yet been reported.

In this study, the PAD from *Bacillus amyloliquefaciens* was explored for the surface display on *S. cerevisiae*. Simultaneously, the PAD expressed in *Pichia pastoris* was introduced to compare the enzymatic property and tolerance to the brewing conditions. Subsequently, the surface displayed PAD was added to blueberry wine to test its ability to enhance vinylphenolic pyranoanthocyanins. Our study demonstrated a promising solution for maintaining the high enzyme activity during the brewing process.

2. Materials and methods

2.1. Blueberry juice, strains, plasmids, and chemicals

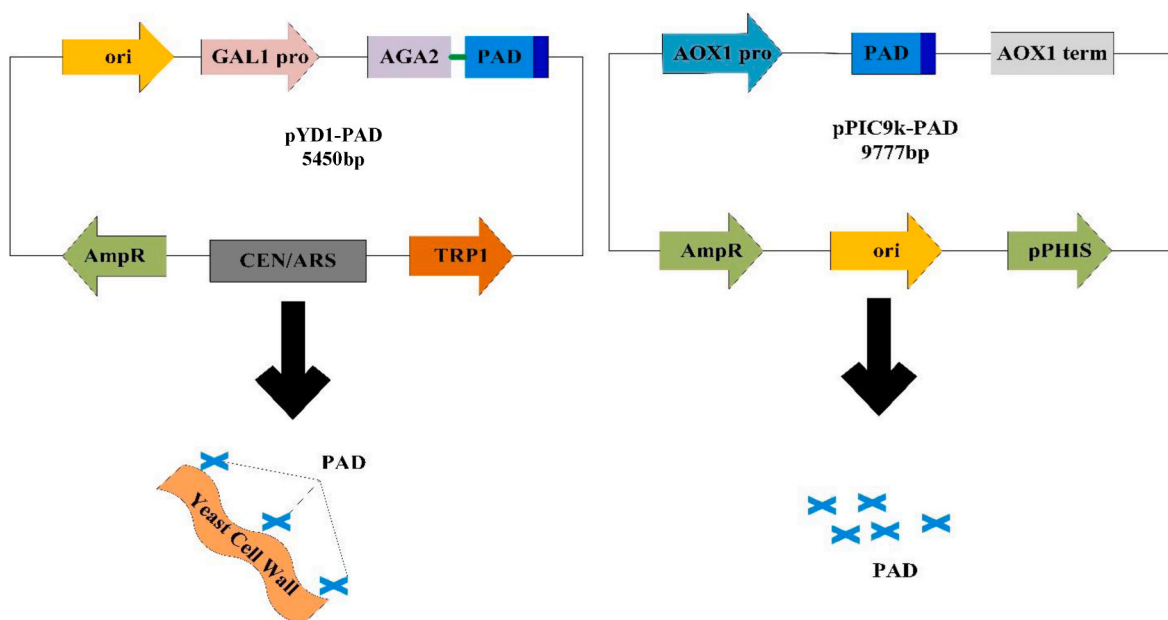
Concentrated blueberry juice was provided by Kweichow Moutai Ecological Agriculture Industry Development Co., Ltd. (Guizhou, China). It was made from rabbit-eye blueberries from Kaili (Guizhou, China) through pulping, enzymolysis, centrifugation, concentration, and sterilization on an industrial scale. The anthocyanin content in blueberry juice detected by Key Laboratory of Carbohydrate Chemistry and Biotechnology is shown in Table S1 (Zhou et al., 2024). The cloning host *Escherichia coli* JM109, expression strain *P. pastoris* GS115, and expression vector pPIC9K were stored in Key Laboratory of Carbohydrate Chemistry and Biotechnology. The expression strain *S. cerevisiae*

EBY100 and expression vector pYD1 were generously provided by South China Agricultural University. The gene used in this experiment was the PAD from *B. amyloliquefaciens* (GenBank accession number YP_003921894.1). Anti-DDDDK Tag Mouse Monoclonal Antibody was purchased from Abbkine (California, USA), FITC AffiniPure Goat Anti-Mouse IgG from Earthox (California, USA), Yeast Competent Cell Preps Kit from Sango Biotech (Shanghai, China), lactose from Macklin Biochemical (Shanghai, China), acid hydrolyzed casein from Macklin Biochemical (Shanghai, China), and yeast nitrogen base from Sango Biotech (Shanghai, China).

2.2. Construction and expression of the recombinant proteins

The construction of recombinant plasmids (pYD1-PAD and pPIC9K-PAD) was shown in Scheme 1. The flexible linker -DYKDDDDK- was used between AGA2 and PAD, the Flag tag was used after PAD. The PAD gene sourced from *B. amyloliquefaciens* was synthesized by GENEWIZ (China). Primers were designed to add the homology arms at both ends of the target gene and plasmid. Plasmids pYD1-PAD and pPIC9K-PAD were constructed by ligating the target gene to the linearized plasmid through the Seamless Cloning Kit (Sinopharm, Shanghai, China). The primers used above was shown in Table S2.

The constructed expression plasmid was transformed into the clonal strain JM109. The recombinants were spread on the LB solid plates containing ampicillin at $100 \mu\text{g mL}^{-1}$. Single colonies were picked for PCR verification and the plasmids were extracted after successful verification. The correctly validated plasmids were transformed into *S. cerevisiae* EBY100 and *P. pastoris* GS115 by a Micro Pulser (Bio-Rad, USA), in which the plasmid pPIC9K-PAD were linearized by single digestion with the enzyme SacI. A single colony of *P. pastoris* GS115 was picked from the MD plate and cultured in YPD at 30°C for 24 h in a shaker of 200 rpm. Then, the culture was inoculated into BMGY with 2% inoculum and cultured for 24 h at 30°C , shaking at 200 rpm. The final culture was added with 1% methanol at an interval of 24 h and induced at 28°C for 4 days. *S. cerevisiae* EBY100 was incubated at 30°C overnight in the YNB-CAA medium containing 2% (w/v) glucose, shaking at 220 rpm. The yeast culture was centrifuged at 4000 rpm for 5 min (SL40R TX-1000, Thermo Scientific, Germany), and the cell pellets were resuspended in the 2% (w/v) galactose YNB-CAA solution. The $\text{OD}_{600\text{nm}}$ value was adjusted to 1 and the culture was induced for 48 h at 20°C ,



Scheme 1. Diagram of the plasmids pYD1-PAD and pPIC9K-PAD. The flexible linker -DYKDDDDK- between AGA2 and PAD was shown in green, and the Flag tag after PAD was shown in blue.

shaking at 220 rpm.

2.3. Primary screening of PAD activity in yeast display cells

The primary screening of yeast with PAD activity was conducted following the protocol described by Escibano et al. with some modifications (Escibano et al., 2017). In the 5 mM ferulic acid solution containing 0.1% (w/v) bromocresol violet, the enzyme solution was added for reaction. Samples were taken at 0 min, 5 min, 10 min, 20 min, 40 min, and 60 min during the reaction process, and PAD activity can be detected by a color shift from yellow (pH = 5.2) to purple (pH = 6.8) due to a change in pH.

2.4. SDS-PAGE analysis

SDS-PAGE analysis was performed in a 12% (w/v) polyacrylamide gel in accordance with the method described by Laemmli (1970), with brief modifications. The crude enzyme samples mixed with the same volume of loading buffer were boiled at 100 °C for 4 min and subsequently subjected to the SDS-PAGE analysis. The gel was stained with Coomassie Brilliant Blue R-250 and destained with the destain solution (2.5% methanol, 10% acetic acid) for 3–5 h.

2.5. Immunofluorescence assay

Localization of displayed PAD was analyzed by indirect immunofluorescence assay. The harvested EBY100 whole cells displayed PAD were re-suspended in phosphate-buffered saline (PBS, pH 6.8) supplemented with 1 mg/mL bovine serum albumin (BSA) and treated with the primary antibody anti-Flag-tag mouse monoclonal antisera (1:500) overnight at 4 °C. Subsequently, these EBY100 whole cells were exposed to the fluorescein isothiocyanate (FITC)-conjugated goat anti-mouse second antibody (1:500) for an hour in darkness, followed by washing 3 times with PBS. One drop of cell suspension was loaded on a glass slide for the confocal microscopy analysis (Leica, Germany). In the same manner, the immunolabeling of EBY100 whole cells that did not display PAD was used as the control (Xu et al., 2020).

2.6. Analysis of enzymatic properties and tolerance to the winemaking conditions

The standard assay mixture contained 0.8 mL of 200 mM Na₂HPO₄-citric acid buffer (pH 6.0), 0.1 mL of 50 mM ferulic acid, and 0.1 mL of crude enzyme solution in 10-mL glass tubes with screw caps (Teflon seals). The reaction mixture was incubated at 37 °C for 15 min before being terminated by adding 2 mL of methanol. The products formed were quantified by high-performance liquid chromatography (HPLC). One unit of enzymatic activity was defined as the enzyme required for the production of 1 μmol of 4-vinyl derivatives per minute. The substrate specificity of PAD toward various hydroxycinnamic acids (*p*-Coumaric, ferulic, caffeic, sinapic acid) was measured at 37 °C (pH 6.0), as described above. Protein content determination of the supernatant was carried out using the Bradford method (Bradford, 1976), with bovine serum albumin (BSA) as the standard.

$$\text{The activity of PAD (IU/mg)} = V_2X/CV_1T \quad (1)$$

where V_1 denotes the quantity of the enzyme solution added, X represents the content of the 4-vinylguaiaicol calculated from the standard curve, V_2 denotes the final volume of the enzymatic reaction system, T represents the reaction time of the enzyme, and C represents the concentration of protein.

2.7. HPLC analysis of 4-vinyl derivatives

Hydroxycinnamic acids and the 4-vinyl derivatives in both the

organic solvent and N₂HPO₄-citric acid buffer phases were analyzed by HPLC (1260 Infinity, Agilent, USA) equipped with a ZORBAX-SB C18 (4.6 × 150 mm, 5 μm in diameter, Agilent, USA) column, a quat pump, and a DAD detector (1260 Infinity, Agilent). The mobile phase acetic acid (0.1%)-methanol (60:40) was used at a flow rate of 1 mL min⁻¹ at 30 °C. The injection volume for all samples was 20 μL. The detection wavelength was set at 280 nm (Hu et al., 2015). The standard curve was plotted by performing linear regression analysis on the peak area of each concentration, using the concentration of the 4-vinylguaiaicol (4-VG) standard sample as the abscissa and the peak area as the ordinate (Fig. S1). It showed the good linear relationship between the peak area and the concentration of the 4-VG solution in the range of 0 mg L⁻¹ to 5 mg L⁻¹.

2.8. Fermentation simulation of blueberry wine

The concentrated blueberry juice was diluted with water in a 1:3 ratio. Subsequently, sucrose and sodium bicarbonate were added to adjust the pH to 3.3 and the sugar content to 20 °Brix. Yeast was inoculated into blueberry juice in 250 mL Erlenmeyer flasks at 10⁶ CFU/mL (Liu et al., 2019).

Both EBY100 whole cells displayed PAD and EBY100 without PAD were subjected to independent fermentation to compare their respective effects.

2.9. LC-MS detection of pyranoanthocyanins

The identification of pyranoanthocyanins was conducted using a MALDI SYNAPT Q-TOF MS system (Water Acquity UPLC, MS, US). The mobile phase A was the water solution of 0.1% formic acid, while the mobile phase B was the acetonitrile solution. A gradient elution was employed, the flow rate was set at 0.3 mL min⁻¹, and the detection wavelength was 520 nm. The column temperature was set at 45 °C, and the sample injection volume was 5 μL. The gradient elution program was 0–40 min, B from 0 to 30%; 40–45 min, B from 30% to 80%; 45–50 min, B from 80% to 100%; 50–55 min, B from 100% to 0. The liquid chromatography column BEH C18 (2.1 × 150 mm, 1.7 μm) was used for analysis. Mass spectrometry conditions were sheath gas 40 psi, auxiliary gas 10 psi, ion spray voltage +3500 V, temperature 400 °C; ion transfer tube temperature 100 °C. The MassLynx V4.1 was used to analyze the data obtained (Zhou et al., 2024).

2.10. Statistical analysis

Statistical analysis was conducted using SPSS 26.0 software. Each assay was performed in triplicate, and the results were presented as mean values with corresponding standard deviations. To identify statistically significant differences, analysis of variance followed by Tukey's test was utilized with a significance level set at $p \leq 0.05$.

3. Results and discussion

3.1. Surface display of PAD on *S. cerevisiae*

The pYD1-PAD plasmid was spiked with a Flag tag, and successful expression of the AGA2-PAD fusion protein would emit green fluorescence under irradiation of green light wavelengths through the recognition effect of anti-Flag tag antibody and FITC anti-mouse IgG antibody. Immunofluorescence reaction was performed to detect whether the AGA2-PAD fusion protein was successfully displayed on the surface of *S. cerevisiae* (Fig. 1A). Based on imaging, it was evident that EBY100/PYD-PAD cells exhibited green fluorescence on their surface, while the EBY100-PYD control did not. EBY100/PYD-PAD cells with successful surface display were added into a ferulic acid solution containing 0.1% bromocresol violet at a concentration of 5 mM. The color of the solution was recorded in 0, 5, 10, 20, 40, and 60 min during the reaction

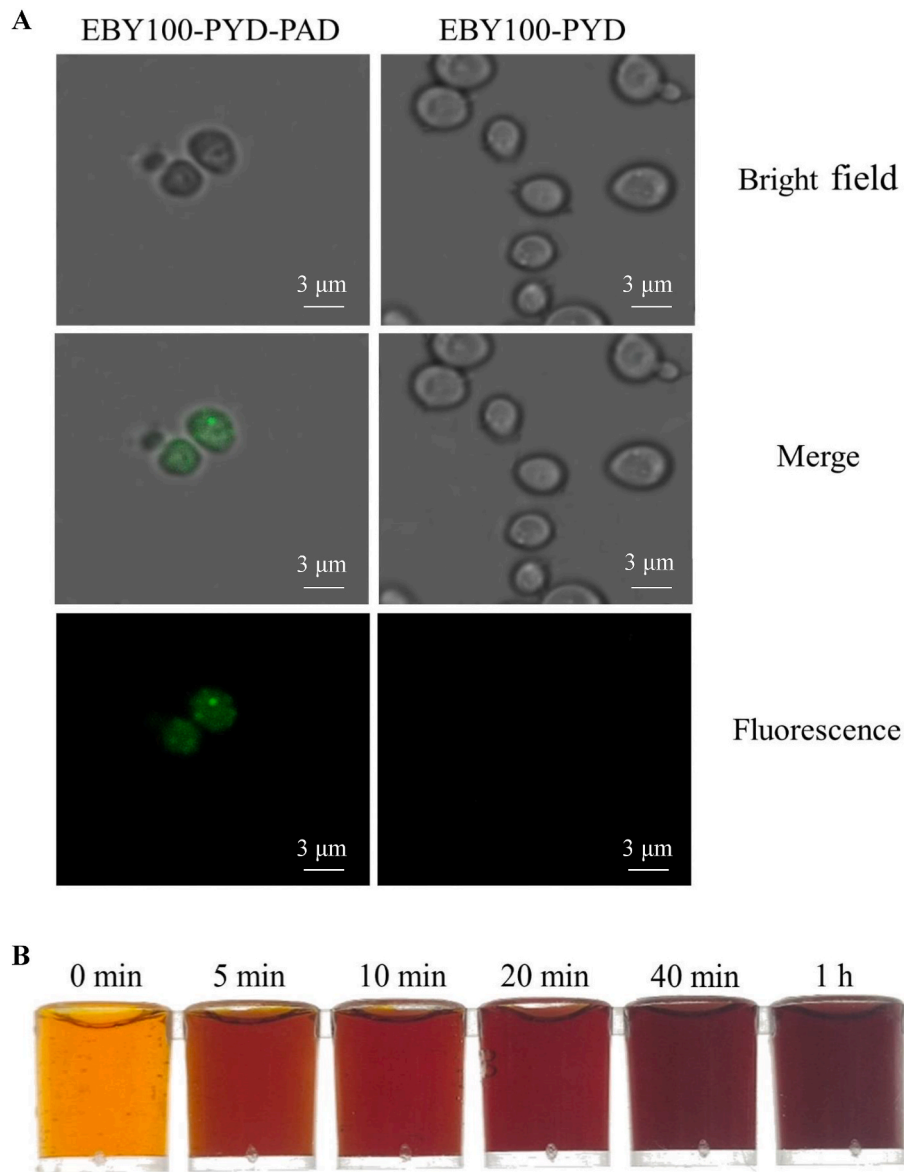


Fig. 1. Surface display of PAD on *S. cerevisiae* strains with the pYD1-PAD and pYD1 plasmids. (A), fluorescence detection under laser confocal microscopy using anti-Flag tag antibodies and FITC-conjugated anti-mouse IgG antibodies for identification. (B), color reaction of the solution of ferulic acid containing bromocresol purple with EBY100/PYD-PAD cells.

(Fig. 1B). The solution color turned a light red in 5 min, further deepened in 10 and 20 min, and became light purple in 40 min. After 1 h of the reaction, the color did not change significantly. These results indicate successful display of PAD on the surface of the *S. cerevisiae* EBY100 cells.

3.2. Expression of PAD by *P. pastoris*

The supernatant of fermentation broth of the GS115-pPIC9K-PAD recombinant strain was subjected to SDS-PAGE gel electrophoresis. The molecular weight of the recombinant PAD was approximately 19.8 KD (Table S3). The SDS-PAGE gel analysis indicated the PAD gene was successfully expressed in *P. pastoris* (Fig. 2A). Moreover, the fermentation supernatant of the recombinant strains GS115-pPIC9K-PAD and GS115-pPIC9K was added into 5 mM ferulic acid solution containing 0.1% bromocresol violet. After 1 h reaction, the supernatant of GS115-pPIC9K-PAD significantly altered the color of the solution from yellow to purple (Fig. 2B). Conversely, the supernatant of *P. pastoris* GS115-pPIC9K did not affect the color of the solution. The results indicated

the PAD gene was successfully expressed by *P. pastoris* GS115 and the PAD activity is very evident.

3.3. Enzymatic properties and tolerance to winemaking conditions

To evaluate the optimal temperature and stability of surface-display PAD (SDPAD) and PAD, their enzyme activities were measured at different temperatures (Fig. 3A) and after incubation for 45 min at the corresponding temperatures (Fig. 3B). The results showed that the optimal temperature for SDPAD was 45 °C, whereas it was 35 °C for PAD (Fig. 3A). At 55 °C, the relative enzyme activity of SDPAD was 93.16%, while for PAD it was only 50.52%. Moreover, SDPAD had significantly higher enzyme activity than PAD when the temperature ranging from 50 °C to 60 °C ($p < 0.05$). The temperature stability indicated that both SDPAD and PAD had about 80% of the relative activity when incubated for 45 min at the temperatures 4°C–45 °C (Fig. 3B). Although there was a substantial decrease in their activity at 45°C–65 °C, SDPAD still exhibited higher stability than PAD. These findings indicate that the surface display treatment has largely enhanced the tolerance of PAD to

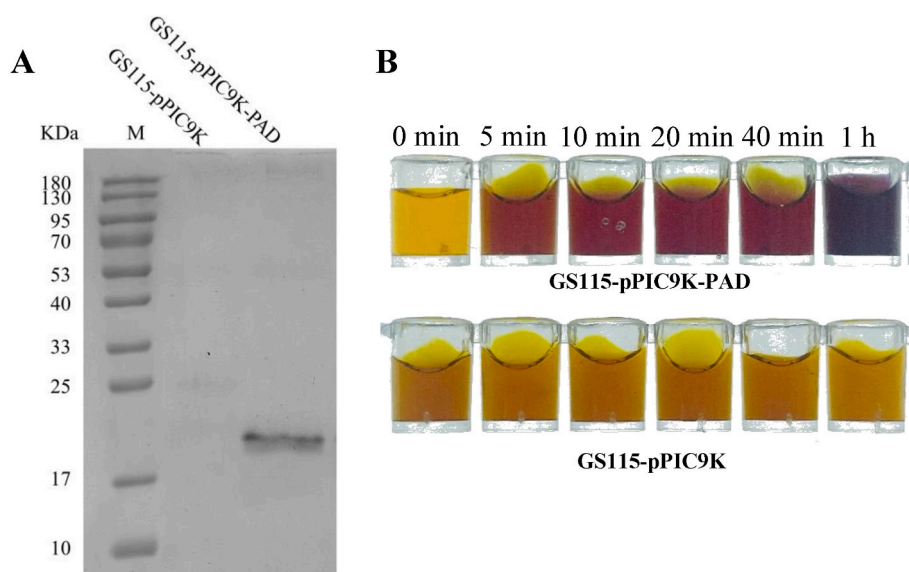


Fig. 2. Identification of expression of PAD in *P. pastoris*. (A), identification of the protein PAD by SDS-PAGE. (B), color reaction of the solution of ferulic acid containing bromocresol purple with the fermentation supernatant of the recombinants pPIC9K-PAD and pPIC9K.

temperature.

The optimal pH and stability of SDPAD and PAD were also evaluated at different pH and after incubation for 45 min at each pH conditions. The optimal pH for PAD was 6 and the relative enzyme activity was consistently above 80% when pH ranging from 5 to 7, with its catalytic activity completely losing at pH 3 (Fig. 3C). In contrast, the optimal pH for SDPAD was 5 and the enzyme activity remained 80% at pH 3–6 After 45 min of incubation at pH 3–4, SDPAD maintained over 60% of enzyme activity, whereas PAD almost lost its catalytic activity (Fig. 3D). These findings indicate that surface display treatment could efficiently improve the tolerance of PAD to acidic conditions.

To determine whether or not surface display can enhance the tolerance of PAD to ethanol, the activity of SDPAD and PAD was tested at different ethanol concentrations (Fig. 3E). It is evident that the residual enzyme activity of SDPAD and PAD exhibited a negative correlation with the increase of ethanol concentrations. The residual enzyme activity of SDPAD and PAD exhibited no significant difference at the ethanol concentrations of 0–25%, indicating that surface display cannot enhance the tolerance of PAD to ethanol.

To evaluate the effectiveness of continuous production, the stability and reusability of the enzyme are crucial. Thus, the enzyme SDPAD was stored at 4 °C and its activity was re-evaluated every 24 h (Fig. 3F). Within the first four recycles, the residual enzyme activity remained 95.76%, 93.55%, 88.19% and 88.16%, respectively. Impressively, SDPAD still maintained over 88% of its enzyme activity after five cycles, exhibiting an outstanding stability and reusability.

To further explain why surface display can enhance the tolerance and stability of PAD, we performed the structural prediction analysis (Fig. S3). As a result, there is a fusion between PAD and the yeast cell wall, enabling SDPAD exhibit a modified spatial structure with more α -helices and less β -folding, compared to PAD. Additionally, the protective effect of the yeast cell wall on the enzyme would be another cause. Yeast surface-displayed proteins act as whole-cell biocatalysts and can self-immobilize on microbial surfaces, which eliminates the requirement for complex purification, immobilization, and recycling, and thus enhancing enzyme tolerance and stability (Liu et al., 2014). A recent study also showed that exhibiting glucosidase on the surface of *S. cerevisiae* to amplify wine aroma significantly enhanced the enzyme's resilience to low pH, ethanol concentration, and high glucose concentration (Zhang et al., 2019).

3.4. Catalytic activity of SDPAD towards different substrates

The substrate specificity of SDPAD was systematically determined using p-Coumaric acid (pCA), ferulic acid (FA), caffeic acid (CA) and sinapic acid (SA) (Fig. 4A). After 40 min reaction, the conversion rates of pCA and FA reached up to 80%, whereas after 1 h the conversion rates of CA and SA were only 60% and 24%, respectively. These findings indicate that SDPAD exhibits the highest affinity to pCA and FA, which is consistent with the previous study (Jung et al., 2013). Based on the analysis of substrate structures (Fig. 4B), it is hypothesized that the presence of two methoxyl groups on the benzene ring of the SA molecule results in a larger molecular volume than others, which probably causes a spatial site-blocking effect on the enzyme's active center of SDPAD (Parada-Fabián et al., 2019). The presence of methoxyl and oxhydroxyl groups in FA and only one methoxyl group in pCA might imply the existence of a better affinity to SDPAD (Fig. 4B). Our findings will help comprehensively understand the enzyme's catalytic properties and the molecular mechanisms for substrate recognition and binding.

3.5. Identification of pyranoanthocyanins by LC-MS

To determine the production of pyranoanthocyanins, the LC-MS analysis was employed to compare the components of blueberry juice before and after fermentation. There was an obvious absorption peak at 18–20 min in the blueberry wine fermented by SDPAD, but it was not evident in the blueberry juice and blueberry wine fermented by EBY100 without PAD (Fig. 5A). Further identification of the molecules of the potential components at this interval was carried out by the mass spectrometry analysis (Fig. 5B). The results demonstrated that the product present at 18.08 min had the m/z values of 625.17 (100%), 626.18 (34.4%) and 627.69 (8.5%), which aligned with the molecular ion peak characterization of petunidin-3-O-glucoside-4-vinylguaiacol ($C_{31}H_{29}O_{14}^+$) (He et al., 2012). The compound present at 18.41 min had the m/z values of 595.13 (100%), 596.15 (33.3%) and 597.15 (8.0%) consistent with the molecular ion peak characterization of petunidin-3-O-glucoside-4-vinylphenol ($C_{30}H_{27}O_{13}^+$) (He et al., 2012). Moreover, the chemical at 18.97 min exhibited the m/z values of 639.18 (100%), 640.19 (34.6%), and 641.18 (9.0%), which aligned with the molecular ion peak characterization of malvidin-3-O-glucoside-4-vinylguaiacol ($C_{32}H_{31}O_{14}^+$) (Hayasaka and Asenstorfer, 2002). Therefore, three more vinylphenolic pyranoanthocyanins were detected in

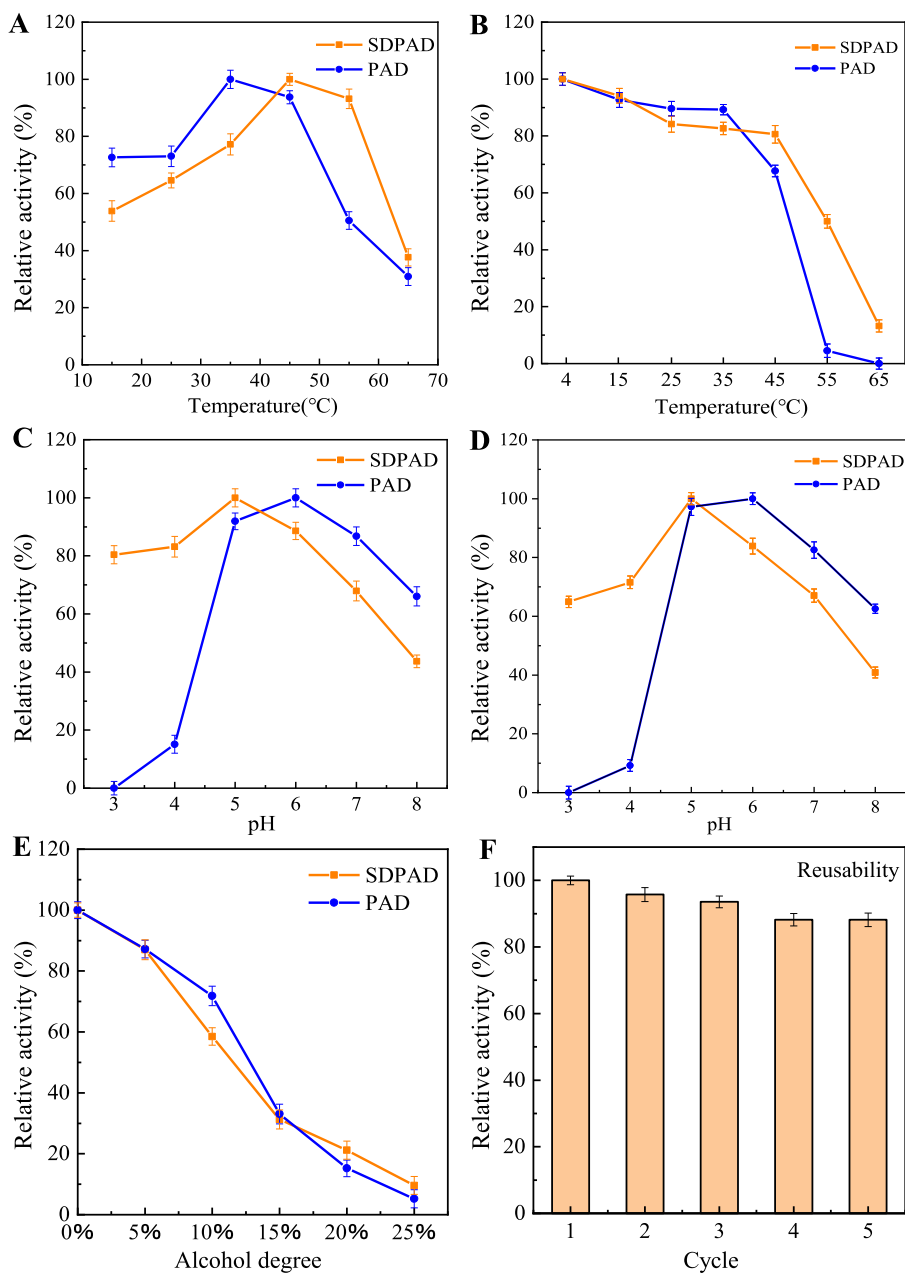


Fig. 3. Comparison of the enzyme properties between SDPAD and PAD. (A) optimal pH, (B) pH tolerance, (C) optimal temperature, (D) thermal stability, (E) ethanol tolerance, and (F) reusability of the SDPAD for 5 cycles. The catalytic activity of the first cycle was defined as 100%.

blueberry wine fermented with SDPAD compared to blueberry juice.

Previous studies suspected that the formation of vinylphenolic pyranoanthocyanins becomes more difficult as the molecular size of the substitution at C3 increases, whereas pentosyl and monosaccharoside (smaller) substitutions are more favorable for the formation of pyranoanthocyanins than hexosyl or disoside substitutions (Farr et al., 2018). This may explain why only monoglycoside anthocyanins were converted to vinylphenolic pyranoanthocyanins in our study. Moreover, the degradation rate of pyranoanthocyanins is lower than that of their corresponding free anthocyanin monomers and the formation of polymerized anthocyanins helps maintain the color of the fruit wine, although they might change the flavor (He et al., 2012; Monagas et al., 2005).

3.6. Analysis of the vinylphenolic pyranoanthocyanins formation

Three vinylphenolic pyranoanthocyanins were identified in blueberry wine fermented with SDPAD: petunidin-3-O-glucoside-4-vinylguaiaicol, petunidin-3-O-glucoside-4-vinylphenol, and malvidin-3-O-glucoside-4-vinylguaiaicol. Among these, one is formed by malvidin-3-O-glucoside and 4-vinylguaiaicol, while the other two are formed by petunidin-3-O-glucoside in conjunction with 4-vinylphenol and 4-vinylguaiaicol, respectively (Fig. 6).

Previous studies indicated that in the formation of vinylphenolic pyranoanthocyanins, the concentration of 4-vinyl derivatives or hydroxycinnamic acids is more important than the concentration of anthocyanins (Akdemir et al., 2019; Rentzsch et al., 2007). Hydroxycinnamic acids in the blueberry juice, including caffeic acid, ferulic acid, p-Coumaric acid, and snapic acid, account for 64% of the total phenolic acids (Zhou et al., 2024). Therefore, there is potentially

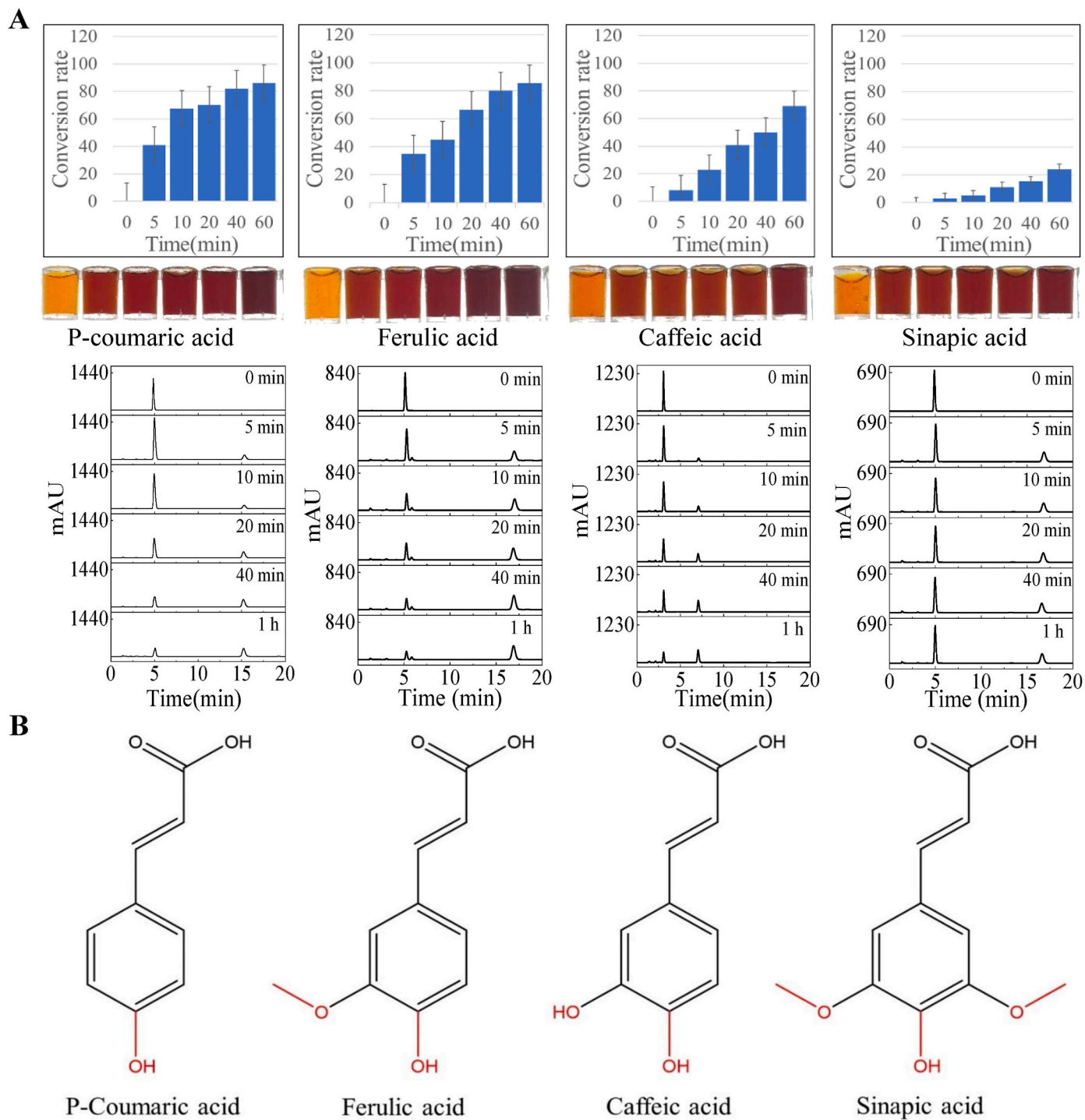


Fig. 4. Conversion rate of four hydroxycinnamic acids catalyzed by SDPAD. (A) monitoring of the conversion process by HPLC and (B) structural formula of the substrates. Color changes were shown below the column chart.

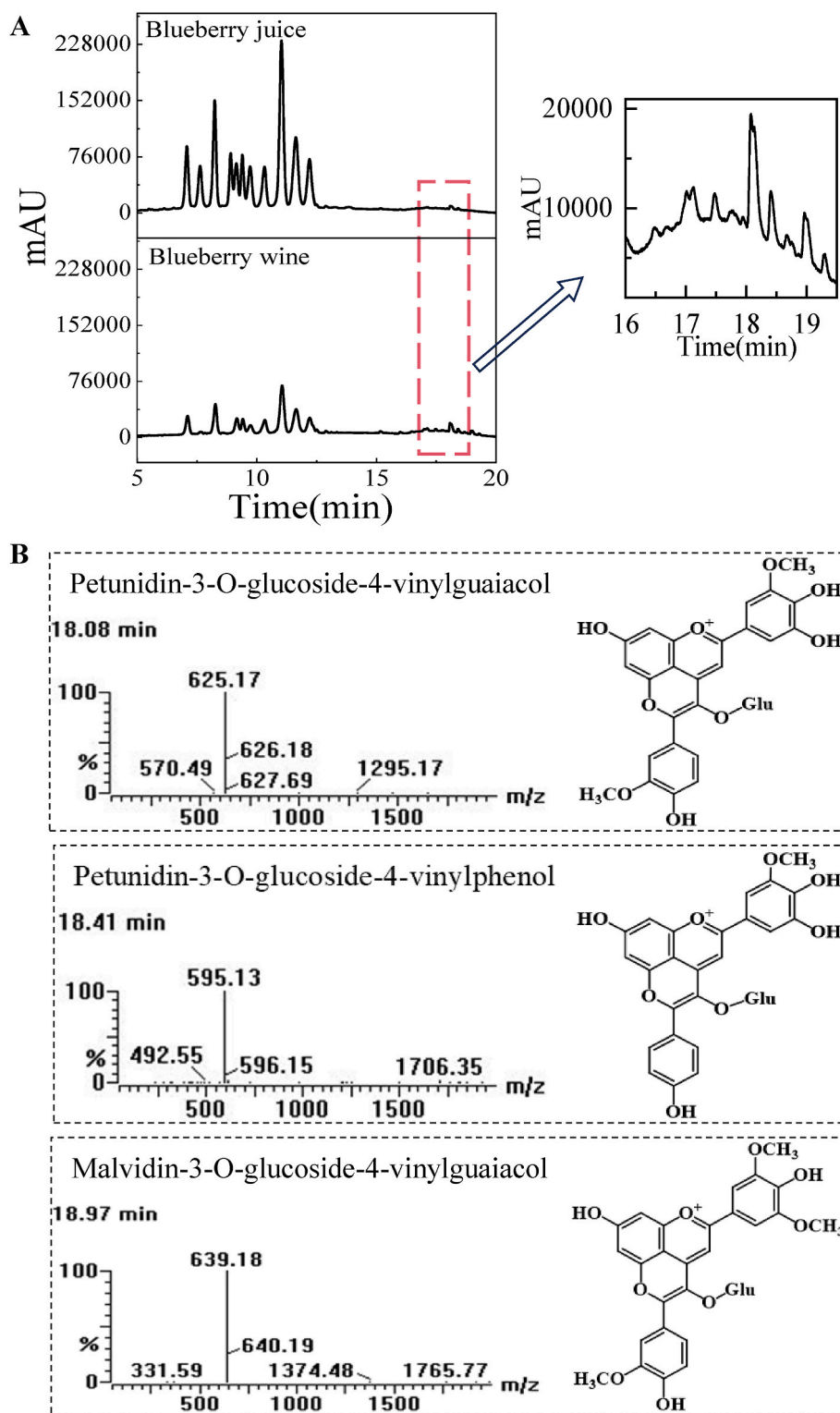


Fig. 5. Identification of the pyranoanthocyanins in blueberry juice before and after fermentation. (A) HPLC spectrum of the potential vinylphenolic pyranoanthocyanins, and (B) the ion spectra and structural formulas of three vinylphenolic pyranoanthocyanins.

sufficient precursor material available to ensure the formation of vinylphenolic pyranoanthocyanins. Our study on the “Catalytic activity of SDPAD towards different substrates” demonstrated that SDPAD exhibited the highest relative enzyme activity for converting ferulic acid to 4-vinylguaiacol, followed by converting p-Coumaric acid to 4-vinylphenol. The three detected vinylphenolic pyranoanthocyanins were all found to be conjugated with either 4-vinylguaiacol or 4-vinylphenol,

which to some extent correlates with the findings of our study on the “Catalytic activity of SDPAD towards different substrates”.

4. Conclusion

This study demonstrated the feasibility of enzyme surface display technology for performance enhancement of phenolic acid

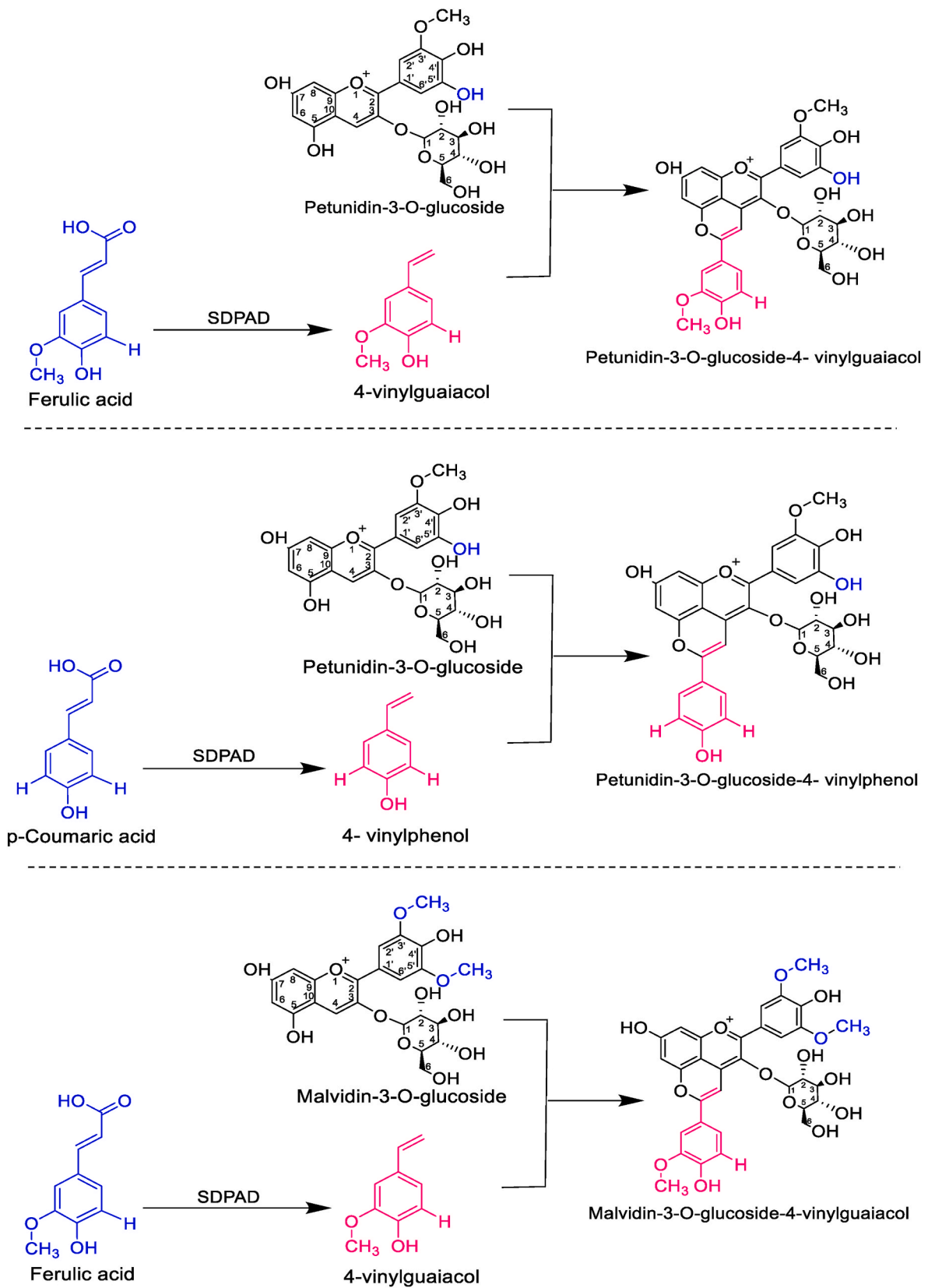


Fig. 6. The vinylphenolic pyranoanthocyanins formed in blueberry wine fermented with SDPAD.

decarboxylase (PAD) on the surface of *S. cerevisiae*. To our knowledge, this is the first time to introduce the surface display of PAD on the brewing yeast to increase the content of vinylphenolic pyranoanthocyanins in fruit wine and improve the color stability of fruit wine. Notably, surface displayed PAD (SDPAD) exhibited a better thermal stability, pH resilience and ethanol endurance, compared to PAD. SDPAD has been proved to be an effective means of facilitating the generation of vinylphenolic pyranoanthocyanins during the blueberry wine production process. Our study will advance the fermentation process of the fruit-based wines, especially for the color stability.

CRedit authorship contribution statement

Huaili Deng: Conceptualization, Methodology, Software, Investigation, Data curation, Writing – original draft, Funding acquisition, Resources. **Qiuya Gu:** Writing – review & editing. **Xiaobin Yu:** Funding acquisition, Resources, Data curation. **Jianli Zhou:** Funding acquisition, Resources, Supervision. **Xiaobo Liu:** Conceptualization, Methodology, Data curation, Writing – review & editing.

Declaration of competing interest

The authors declare that they have no known competing financial interests or personal relationships that could have appeared to influence the work reported in this paper.

Data availability

Data will be made available on request.

Acknowledgments

This project was financially supported by the National Natural Science Foundation of China (Grant No. 32360228), Guizhou Provincial Science and Technology Foundation (ZK [2022] General Project 190), and Guizhou University Natural Science Special Project, (No. [2023] 21).

Appendix A. Supplementary data

Supplementary data to this article can be found online at <https://doi.org/10.1016/j.crfs.2024.100730>.

References

- Akdemir, H., Silva, A., Zha, J., Zagorevski, D.V., Koffas, M.A.G., 2019. Production of pyranoanthocyanins using *Escherichia coli* co-cultures. *Metab. Eng.* 55, 290–298. <https://doi.org/10.1016/j.ymben.2019.05.008>.
- Benito, S., Morata, A., Palomero, F., González, M., Suárez-Lepe, J., 2011. Formation of vinylphenolic pyranoanthocyanins by *Saccharomyces cerevisiae* and *Pichia guilliermondii* in red wines produced following different fermentation strategies. *Food Chem.* 124 (1), 15–23. <https://doi.org/10.1016/j.foodchem.2010.05.096>.
- Bradford, M.M., 1976. A rapid and sensitive method for the quantitation of microgram quantities of protein utilizing the principle of protein-dye binding. *Anal. Biochem.* 72 (1–2), 248–254. <https://doi.org/10.1006/abio.1976.9999>.
- Çelik, E., Çalik, P., 2012. Production of recombinant proteins by yeast cells. *Biotechnol. Adv.* 30 (5), 1108–1118. <https://doi.org/10.1016/j.biotechadv.2011.09.011>.
- De Freitas, V., Mateus, N., 2011. Formation of pyranoanthocyanins in red wines: a new and diverse class of anthocyanin derivatives. *Anal. Bioanal. Chem.* 401 (5), 1463–1473. <https://doi.org/10.1007/s00216-010-4479-9>.
- Escribano, R., Gonzalez-Arenzana, L., Garijo, P., Berlanas, C., Lopez-Alfaro, I., Lopez, R., Rosa Gutierrez, A., Santamaria, P., 2017. Screening of enzymatic activities within different enological non-*Saccharomyces* yeasts. *J. Food Sci. Technol.-Mysore* 54 (6), 1555–1564. <https://doi.org/10.1007/s13197-017-2587-7>.

- Farr, J.E., Sigurdson, G.T., Giusti, M.M., 2018. Influence of cyanidin glycosylation patterns on carboxypyrananthocyanin formation. *Food Chem.* 259, 261–269. <https://doi.org/10.1016/j.foodchem.2018.03.117>.
- Gao, Y., Wang, X., Ai, J., Huang, W., Zhan, J., You, Y., 2023. Formation of vinylphenolic pyranoanthocyanins by selected indigenous yeasts displaying high hydroxycinnamate decarboxylase activity during mulberry wine fermentation and aging. *Food Microbiol.* 113, 104272. <https://doi.org/10.1016/j.fm.2023.104272>.
- Hayasaka, Y., Asenstorfer, R.E., 2002. Screening for potential pigments derived from anthocyanins in red wine using nano-electrospray tandem mass spectrometry. *J. Agric. Food Chem.* 50 (4), 756–761. <https://doi.org/10.1021/jf010943v>.
- He, F., Liang, N.-N., Mu, L., Pan, Q.-H., Wang, J., Reeves, M.J., Duan, C.-Q., 2012. Anthocyanins and their variation in red wines II. Anthocyanin derived pigments and their color evolution. *Molecules* 17 (2), 1483–1519. <https://doi.org/10.17221/189/2016-CJFS>.
- Hu, H., Li, L., Ding, S., 2015. An organic solvent-tolerant phenolic acid decarboxylase from *Bacillus licheniformis* for the efficient bioconversion of hydroxycinnamic acids to vinyl phenol derivatives. *Appl. Microbiol. Biotechnol.* 99 (12), 5071–5081. <https://doi.org/10.1007/s00253-014-6313-3>.
- Jung, D.-H., Choi, W., Choi, K.-Y., Jung, E., Yun, H., Kazlauskas, R.J., Kim, B.-G., 2013. Bioconversion of p-coumaric acid to p-hydroxystyrene using phenolic acid decarboxylase from *B. amyloliquefaciens* in biphasic reaction system. *Appl. Microbiol. Biotechnol.* 97 (4), 1501–1511. <https://doi.org/10.1007/s00253-012-4358-8>.
- Kondo, A., Ueda, M., 2004. Yeast cell-surface display—applications of molecular display. *Appl. Microbiol. Biotechnol.* 64 (1), 28–40. <https://doi.org/10.1007/s00253-003-1492-3>.
- Laemmli, U.K., 1970. Cleavage of structural proteins during the assembly of the head of bacteriophage T4. *Nature* 227 (5259), 680–685. <https://doi.org/10.1038/227680a0>.
- Lentz, M., 2018. The impact of simple phenolic compounds on beer aroma and flavor. *Fermentation* 4 (1), 20. <https://doi.org/10.3390/fermentation4010020>.
- Liu, F., Li, S., Gao, J., Cheng, K., Yuan, F., 2019. Changes of terpenoids and other volatiles during alcoholic fermentation of blueberry wines made from two southern highbush cultivars. *Lwt* 109, 233–240. <https://doi.org/10.1016/j.lwt.2019.03.100>.
- Liu, Y., Zhang, T., Qiao, J., Liu, X., Bo, J., Wang, J., Lu, F., 2014. High-yield phosphatidylserine production via yeast surface display of phospholipase D from *Streptomyces chromofuscus* on *Pichia pastoris*. *J. Agric. Food Chem.* 62 (23), 5354–5360. <https://doi.org/10.1021/jf405836x>.
- Lu, Y., Sun, Y., Foo, L.Y., 2000. Novel pyranoanthocyanins from black currant seed. *Tetrahedron Lett.* 41 (31), 5975–5978. [https://doi.org/10.1016/S0040-4039\(00\)00954-0](https://doi.org/10.1016/S0040-4039(00)00954-0).
- Monagas, M., Bartolomé, B., Gómez-Cordovés, C., 2005. Evolution of polyphenols in red wines from *Vitis vinifera* L. during aging in the bottle: II. Non-anthocyanin phenolic compounds. *Eur. Food Res. Technol.* 220, 331–340. <https://doi.org/10.1007/s00217-004-1109-9>.
- Morata, A., Loira, I., González, C., Escott, C., 2021. Non-*Saccharomyces* as biotools to control the production of off-flavors in wines. *Molecules* 26 (15), 4571. <https://doi.org/10.3390/molecules26154571>.
- Oliveira, J., de Freitas, V., Silva, A.M., Mateus, N., 2007. Reaction between hydroxycinnamic acids and anthocyanin—pyruvic acid adducts yielding new portisins. *J. Agric. Food Chem.* 55 (15), 6349–6356. <https://doi.org/10.1021/jf070968f>.
- Parada-Fabián, J.C., Hernández-Sánchez, H., Méndez-Tenorio, A., 2019. Substrate specificity of the phenolic acid decarboxylase from *Lactobacillus plantarum* and related bacteria analyzed by molecular dynamics and docking. *J. Plant Biochem. Biotechnol.* 28, 91–104. <https://doi.org/10.1007/s13562-018-0466-6>.
- Rentzsch, M., Schwarz, M., Winterhalter, P., 2007. Pyranoanthocyanins – an overview on structures, occurrence, and pathways of formation. *Trends Food Sci. Technol.* 18 (10), 526–534. <https://doi.org/10.1016/j.tifs.2007.04.014>.
- Sheng, X., Lind, M.E., Himo, F., 2015. Theoretical study of the reaction mechanism of phenolic acid decarboxylase. *FEBS J.* 282 (24), 4703–4713. <https://doi.org/10.1111/febs.13525>.
- Sun, J.X., Li, X.H., Luo, H.X., Ding, L.J., Jiang, X.W., Li, X.S., Jiao, R., Bai, W.B., 2020. Comparative study on the stability and antioxidant activity of six pyranoanthocyanins based on malvidin-3-glucoside. *J. Agric. Food Chem.* 68 (9), 2783–2794. <https://doi.org/10.1021/acs.jafc.9b06734>.
- Xu, L., Xiao, X., Wang, F., He, Y., Yang, X., Hu, J., Feng, Z., Yan, Y., 2020. Surface-displayed thermostable *Candida rugosa* lipase 1 for docosahexaenoic acid enrichment. *Appl. Biochem. Biotechnol.* 190 (1), 218–231. <https://doi.org/10.1007/s12010-019-03077-z>.
- Zhang, Y., Min, Z., Qin, Y., Ye, D.-Q., Song, Y.-Y., Liu, Y.-L., 2019. Efficient Display of *Aspergillus niger* β -glucosidase on *Saccharomyces cerevisiae* cell wall for aroma enhancement in wine. *J. Agric. Food Chem.* 67 (18), 5169–5176. <https://doi.org/10.1021/acs.jafc.9b00863>.
- Zhou, J., Tang, C., Zou, S., Lei, L., Wu, Y., Yang, W., Harindintwali, J.D., Zhang, J., Zeng, W., Deng, D., Zhao, M., Yu, X., Liu, X., Qiu, S., Arneborg, N., 2024. Enhancement of pyranoanthocyanin formation in blueberry wine with non-*Saccharomyces* yeasts. *Food Chem.* 438, 137956. <https://doi.org/10.1016/j.foodchem.2023.137956>.